

- TCCCCGGGGCTTCACTACTCGCTGCGT-3' (nucleotides 3 to 23) and PR2, and products were analyzed. A major ~600-bp fragment was isolated from the gel and cloned to generate pSGC5, and the DNA sequence determined.
9. S. F. Yu and M. L. Linial, *J. Virol.* **67**, 6618 (1993).
  10. M. Lochelt, H. Zentgraf, R. M. Flügel, *Virology* **184**, 43 (1991).
  11. D. N. Baldwin and M. L. Linial, unpublished data.
  12. K. O. Netzer, A. Rethwilm, B. Maurer, V. ter Meulen, *J. Gen. Virol.* **71**, 1237 (1990); A. Bartholoma, W. Muranyi, R. M. Flügel, *Virus Res.* **23**, 27 (1992).
  13. S. F. Yu and M. L. Linial, unpublished data.
  14. K. M. Felsenstein and S. P. Goff, *J. Virol.* **62**, 2179 (1988).
  15. Calculation of the number of DNA molecules present in HFV virions was done as follows. An estimated 113 pg of ~12-kb double-stranded DNA was detected from 22 ml of virus supernatant, as determined by Southern blot analysis with pHFV13 plasmid DNA standards. The molecular mass of this ~12-kb double-stranded DNA is about 7.9 × 10<sup>6</sup> g/mol. Therefore, 113 pg of DNA is equal to 8.9 × 10<sup>6</sup> DNA molecules. Particle counts determined by electronic microscopy showed that there were about 5.5 × 10<sup>7</sup> virions present in the 22 ml of viral supernatant. By dividing 8.9 × 10<sup>6</sup> DNA molecules by 5.5 × 10<sup>7</sup> virions, we concluded that there is approximately one DNA molecule present in every six virions. In an independent experiment we found a DNA molecule in every nine virions. In viral preparations harvested after 48 hours, we determined that 1 in 25 to 100 supernatant virions is infectious as measured in the FAB assay.
  16. F. Lori et al., *J. Virol.* **66**, 5067 (1992); D. Trono, *ibid.*, p. 4893.
  17. B. Maurer, H. Bannert, G. Darai, R. M. Flügel, *ibid.* **62**, 1590 (1988).
  18. J. W. Wills and R. C. Craven, *AIDS* **5**, 639 (1991).
  19. R. Marquet, C. Isel, C. Ehresmann, B. Ehresmann, *Biochimie* **77**, 113 (1995).
  20. T. Hatton, S. Zhou, D. N. Standing, *J. Virol.* **66**, 5232 (1992).
  21. R. Bartenschlager and H. Schaller, *EMBO J.* **11**, 3413 (1992); R. C. Hirsch, J. E. Levine, L.-J. Chang, H. E. Varmus, D. Ganem, *Nature* **344**, 552 (1990).
  22. G. H. Wang and C. Seeger, *Cell* **71**, 663 (1992); D. Ganem, J. R. Pollack, J. Tavis, *Infect. Agents. Dis.* **3**, 85 (1994).
  23. M. Nassal and H. Schaller, *Trends Microbiol.* **1**, 221 (1993).
  24. D. Kogel, M. Aboud, R. M. Flügel, *Virology* **213**, 97 (1995).
  25. H. Hahn et al., *J. Gen. Virol.* **75**, 2635 (1994).
  26. A. W. Schliephake and A. Rethwilm, *J. Virol.* **68**, 4946 (1994).
  27. I. A. Wilson et al., *Cell* **37**, 767 (1984).
  28. S. F. Yu, J. Stone, M. L. Linial, *J. Virol.* **70**, 1250 (1996).
  29. We thank M. Groudine and M. Emerman for their critiques of the manuscript and A. Rethwilm for stimulating discussions about the HFV genome. We also thank A. R. and R. Flügel for providing antisera and L. Caldwell and the electron microscopy facility at the Fred Hutchinson Cancer Research Center for particle counts. Supported by NIH grants CA18282 and HL53762 to M.L.L. S.F.Y. was partially supported by a postdoctoral fellowship (F32 CA60357) from the National Cancer Institute.

26 October 1995; accepted 16 January 1996

## HIV-1 Dynamics in Vivo: Virion Clearance Rate, Infected Cell Life-Span, and Viral Generation Time

Alan S. Perelson, Avidan U. Neumann, Martin Markowitz,  
John M. Leonard, David D. Ho\*

A new mathematical model was used to analyze a detailed set of human immunodeficiency virus-type 1 (HIV-1) viral load data collected from five infected individuals after the administration of a potent inhibitor of HIV-1 protease. Productively infected cells were estimated to have, on average, a life-span of 2.2 days (half-life  $t_{1/2} = 1.6$  days), and plasma virions were estimated to have a mean life-span of 0.3 days ( $t_{1/2} = 0.24$  days). The estimated average total HIV-1 production was  $10.3 \times 10^9$  virions per day, which is substantially greater than previous minimum estimates. The results also suggest that the minimum duration of the HIV-1 life cycle in vivo is 1.2 days on average, and that the average HIV-1 generation time—defined as the time from release of a virion until it infects another cell and causes the release of a new generation of viral particles—is 2.6 days. These findings on viral dynamics provide not only a kinetic picture of HIV-1 pathogenesis, but also theoretical principles to guide the development of treatment strategies.

HIV-1 replication in vivo occurs continuously at high rates (1, 2). Ho et al. (1) found that when a protease inhibitor was administered to infected individuals, plasma concentrations of HIV-1 decreased exponentially, with a mean  $t_{1/2}$  of  $2.1 \pm 0.4$  days. Wei et al. (2) and Nowak et al. (3) found essentially identical kinetics of viral decay after the use of inhibitors of HIV-1 protease or reverse transcriptase. The viral decay observed in these studies was a composite of two separate effects: the clearance of free virions from plasma and the loss of virus-producing cells. To under-

stand the kinetics of these two viral compartments more precisely, we closely monitored the viral load in five HIV-1-infected patients after the administration of a potent protease inhibitor. Using a mathematical model for viral dynamics and nonlinear least squares fitting of the data, we obtained separate estimates of the virion clearance rate, the infected cell life-span, and the average viral generation time in vivo.

Ritonavir (4, 5) was administered orally (600 mg twice daily) to five infected patients, whose base-line characteristics are shown in Table 1. After treatment, we measured HIV-1 RNA concentrations in plasma at frequent intervals (every 2 hours until the sixth hour, every 6 hours until day 2, and every day until day 7) by means of an ultrasensitive modification (1, 5) of the branched DNA assay (6). Each patient responded with a similar pattern of viral de-

cay: an initial lag followed by an approximately exponential decline in plasma viral RNA (see Fig. 1 for examples).

After ritonavir was administered, a delay in its antiviral effect was expected because of the time required for drug absorption, distribution, and penetration into the target cells. This pharmacokinetic delay could be estimated by the time elapsed before the first drop in the titer of infectious HIV-1 in plasma (Table 1 and Fig. 1B). However, even after the pharmacokinetic delay was accounted for, a lag of ~1.25 days was observed before the plasma viral RNA concentration fell (Fig. 1). This additional delay is consistent with the mechanism of action of protease inhibitors, which render newly produced virions noninfectious but do not inhibit either the production of virions from already infected cells or the infection of new cells by previously produced infectious virions (7). In our previous study (1), this additional delay was missed because measurements were less frequent (every 3 days), and the results were fitted to a single exponential, which was sufficient to provide minimum estimates of HIV-1 kinetics. In contrast, in the present study, we obtained 15 data points during the first 7 days, which allowed a careful analysis of the results by means of a new mathematical model of viral kinetics.

We assumed that HIV-1 infects target cells ( $T$ ) with a rate constant  $k$  and causes them to become productively infected cells ( $T^*$ ). Before drug treatment, the dynamics of cell infection and virion production are represented by

$$\frac{dT^*}{dt} = kVT - \delta T^* \quad (1)$$

$$\frac{dV}{dt} = N\delta T^* - cV \quad (2)$$

A. S. Perelson and A. U. Neumann, Theoretical Division, Los Alamos National Laboratory, Los Alamos, NM 87545, USA.

M. Markowitz and D. D. Ho, Aaron Diamond AIDS Research Center, 455 First Avenue, New York, NY 10016, USA.

J. M. Leonard, Pharmaceutical Products Division, Abbott Laboratories, Abbott Park, IL 60064, USA.

\*To whom correspondence should be addressed.

Dis. 3,  
1. 221  
3. 97  
1. 68,  
1250  
r their  
stim'e also  
and L.  
at the  
part-  
2 and  
ted by  
m the  
roxi-  
viral  
a de-  
cted  
g ab-  
lation  
netic  
time  
er of  
and  
urma-  
ag of  
plas-  
g. 1).  
with  
e in-  
duced  
inhibit  
m al-  
f new  
ctious  
, this  
mea-  
ery 3  
to a  
ent to  
-1 ki-  
study,  
e first  
sis of  
emat-

target  
causes  
1 cells  
amics  
on are

where  $V$  is the concentration of viral particles in plasma,  $\delta$  is the rate of loss of virus-producing cells,  $N$  is the number of new virions produced per infected cell during its lifetime, and  $c$  is the rate constant for virion clearance (8). The loss of infected cells could be the result of viral cytopathicity, immune elimination, or other processes such as apoptosis. Virion clearance could be the result of binding and entry into cells, immune elimination, or nonspecific removal by the reticuloendothelial system.

We assumed that ritonavir does not affect the survival or rate of virion production of infected cells, and that after the pharmacological delay, all newly produced virions are noninfectious. However, infectious virions produced before the drug effect are still present until they are cleared. Therefore, after treatment with ritonavir,

$$\frac{dT^*}{dt} = kV_1 T - \delta T^* \quad (3)$$

$$\frac{dV_1}{dt} = -cV_1 \quad (4)$$

$$\frac{dV_{NI}}{dt} = N\delta T^* - cV_{NI} \quad (5)$$

where  $V_1$  is the plasma concentration of virions in the infectious pool [produced before the drug effect;  $V_1(t=0) = V_0$ ],  $V_{NI}$  is the concentration of virions in the noninfectious pool [produced after the drug effect;  $V_{NI}(t=0) = 0$ ], and  $t = 0$  is the time of onset of the drug effect. In our analyses, we assumed that viral inhibition by ritonavir is 100%, although the model can be generalized for nonperfect drugs (9).

Assuming that the system is at quasi steady state before drug treatment (10) and that the uninfected cell concentration

$T$  remains at approximately its steady-state value,  $T_0$ , for 1 week after drug administration (1, 5), we find from Eqs. 3 through 5 that the total concentration of plasma virions,  $V = V_1 + V_{NI}$ , varies as

$$V(t) = V_0 \exp(-ct) + \frac{cV_0}{c - \delta} \left\{ \frac{c}{c - \delta} [\exp(-\delta t) - \exp(-ct)] - \delta t \exp(-ct) \right\} \quad (6)$$

which differs from the equation derived by Wei *et al.* [(2); see (11)]. Allowing  $T$  to increase necessitates the use of numerical methods to predict  $V(t)$  but does not substantially alter the outcomes of the analyses given below (12).

Using nonlinear regression analysis (Fig. 1), we estimated  $c$  and  $\delta$  for each of the patients by fitting Eq. 6 to the plasma HIV-1 RNA measurements (Table 1) (12). The theoretical curves generated from Eq. 6, using the best-fit values of  $c$  and  $\delta$ , gave an excellent fit to the data for all patients (see Fig. 1 for examples). Clearance of free virions is the more rapid process, occurring on a time scale of hours. Values of  $c$  ranged from 2.06 to 3.81 day<sup>-1</sup>, with a mean of  $3.07 \pm 0.64$  day<sup>-1</sup> (Table 1). The corresponding  $t_{1/2}$  values for free virions ( $t_{1/2} = \ln 2/c$ ) ranged from 0.18 to 0.34 days, with a mean of  $0.24 \pm 0.06$  days (~6 hours). Confirmation of the virion clearance rate was obtained from an independent experiment that measured by quantitative cultures (13) the rate of loss of viral infectivity in plasma for patient 105 (Fig. 1B). The loss of infectious virions occurred by first-order decay, with a rate constant of  $3.0$  day<sup>-1</sup>, which is within the 68% confidence interval of the esti-

mated  $c$  value for that patient (Table 1).

At steady state, the production rate of virus must equal its clearance rate,  $cV$ . Using the estimate of  $c$  and the pretreatment viral concentration  $V_0$ , we obtained an estimate for the rate of virion production before ritonavir administration. Each patient's plasma and extracellular fluid volumes were estimated on the basis of body weight. Total daily virion production and clearance rates ranged from  $0.4 \times 10^9$  to  $32.1 \times 10^9$  virions per day, with a mean of  $10.3 \times 10^9$  virions per day released into the extracellular fluid (Table 1) (14). The rate of loss of virus-producing cells, as estimated from the fit of Eq. 6 to the HIV-1 RNA data, was slower than that of free virions. Values of  $\delta$  ranged from 0.26 to 0.68 day<sup>-1</sup>, with a mean of  $0.49 \pm 0.13$  day<sup>-1</sup>; the corresponding  $t_{1/2}$  values were 1.02 to 2.67 days, with a mean of  $1.55 \pm 0.57$  days (Table 1). A prediction of the kinetics of virus-producing cells can be obtained by solving Eq. 3 (15).

Several features of the replication cycle of HIV-1 in vivo could be discerned from our analysis. Given that  $c$  and  $\delta$  represent the decay rate constants for plasma virions and productively infected cells, respectively, then  $1/c$  and  $1/\delta$  are the corresponding average life-spans of these two compartments. Thus, the average life-span of a virion in the extracellular phase is  $0.3 \pm 0.1$  days, whereas the average life-span of a productively infected cell is  $2.2 \pm 0.8$  days (Table 2). The average viral generation time  $\tau$  is defined as the time from the release of a virion until it infects another cell and causes the release of a new generation of viral particles; hence,  $\tau$  should equal the sum of the average life-span of a free virion and the average life-span of a productively infected cell. This relation,  $\tau$

**Table 1.** Summary of HIV-1 clearance rate, infected cell loss rate, and virion production rate for the five patients. Base-line values are average of measurements taken at days -7, -4, -1, and 0; each virion contains two RNA copies. Pharmacologic delay was estimated from the first drop in plasma infectivity for patients 102, 105, and 107. Delay was estimated by best fit of viral load to Eq.

6 for patients 103 and 104. Lower and upper 68% confidence intervals were calculated by a bootstrap method (22) in which each experiment was simulated 100 times. Total virion production was calculated from plasma and extracellular fluid volumes estimated from body weights, assuming that plasma and extracellular fluid are in equilibrium.

Patient	Base-line values		Pharm. delay (hours)	Estimates from fit of $V(t)$ to plasma viral load								Total virion production ( $10^9$ per day)		
				Virion clearance				Infected cell loss						
	CD4 cells (per mm <sup>3</sup> )	Plasma virions ( $10^3$ per ml)		$c$ (day <sup>-1</sup> )	Confidence interval		$t_{1/2}$ (days)	$\delta$ (day <sup>-1</sup> )	Confidence interval		$t_{1/2}$ (days)			
(1)	102	16	294	2	3.81	1.93	7.03	0.18	0.26	0.24	0.30	2.67	12.9	
	103	408	12	6	2.73	2.04	3.70	0.25	0.68	0.63	0.73	1.02	0.4	
	104	2	52	2	3.68	2.53	6.19	0.19	0.50	0.47	0.54	1.39	2.9	
	105	11	643	6	2.06	1.42	3.76	0.34	0.53	0.48	0.60	1.31	32.1	
	107	412	77	2	3.09	2.56	4.55	0.22	0.50	0.48	0.52	1.39	3.1	
	Mean	170	216	3.6	3.07	2.10	5.05	0.24	0.49	0.46	0.54	1.55	10.3	
(2)	$\pm SD$	196	235	2.0	0.64	0.42	1.34	0.06	0.13	0.13	0.14	0.57	11.7	

$= 1/c + 1/\delta$ , can be shown formally (Table 2). The average value of  $\tau$  for the patients was  $2.6 \pm 0.8$  days (Table 2).

By a heuristic procedure, we found minimal estimates for the average duration of the HIV-1 life cycle and of its intracellular or eclipse phase (from virion binding to the release of the first progeny). The duration of the HIV-1 life cycle,  $S$ , is defined as the time from the release of a virion until the release of its first progeny virus; we estimated  $S$  by the lag in the decay of HIV-1 RNA in plasma (Fig. 1) after the pharmacologic delay (Table 1) is subtracted. The shoulder in the RNA decay curve is explained by the fact that virions produced before the pharmacologic effect of ritonavir are still infectious and capable of producing, for a single cycle, viral particles that would be detected by the RNA assay. Thus, the drop in RNA concentration should begin when target cells interact with drug-affected virions and do not produce new virions. These "missing virions" would first have been produced at a time equal to the minimum time for infection plus the minimum time for production of new progeny. The estimated values for  $S$  were quite consistent for the five patients, with a mean duration of  $1.2 \pm 0.1$  days (Table 2). In steady state,  $1/c = 1/NkT_0$  is the average time for infection (Table 2, legend); if this average time is assumed to be greater than the minimal time for infection, then a minimal estimate of the average duration of the intracellular phase of the HIV-1 life cycle is given by  $S - (1/c) = 0.9$  days (16).

Previous studies that used potent antiretroviral agents to perturb the quasi steady state in vivo provided a crude estimate of the  $t_{1/2}$  of viral decay in which the life-span of productively infected cells could not be separated from that of plasma virions (1, 2). Our results show that the average life-span of a productively infected cell (presumably an activated CD4 lymphocyte) is 2.2 days; thus, such cells are lost with an average  $t_{1/2}$  of  $\sim 1.6$  days (Fig. 2). The life-spans of productively infected cells were not markedly different among the five patients (Table 2), even though individuals with low CD4 lymphocyte counts generally have decreased numbers of virus-specific, major histocompatibility complex class I-restricted cytotoxic T lymphocytes (17).

The average life-span of a virion in blood was calculated to be 0.3 days. Therefore, a population of plasma virions is cleared with a  $t_{1/2}$  of 0.24 days; that is, on average, half of the population of plasma virions turns over approximately every 6 hours (Fig. 2). Because our analysis assumed that the antiviral effect of ritonavir was complete and that target cells did not recover during treatment, our estimates of the virion clearance rate and infected cell loss

rate are minimal estimates (12, 16). Consequently, the true virion  $t_{1/2}$  may be shorter than 6 hours. For example, Nathanson and Harrington (18) found that monkeys clear the Langat virus from their circulation on a time scale of  $\sim 30$  min. Thus, the total number of virions produced and released into the extracellular fluid is at least  $10.3 \times 10^9$  particles per day (14); this rate is about 15 times our previous minimum estimate (1). At least 99% of this large pool of virus is produced by recently infected cells (1, 2) (Fig. 2). At quasi steady state, the virion clearance rate  $cV$  equals the virion production rate  $N\delta T^*$ . Because  $c$  has similar values for all patients studied (Table 1), the degree of plasma viremia is a reflection of the total virion production, which in turn is proportional to the number of productively infected cells  $T^*$  and their viral burst size  $N$ . The average generation time of HIV-1 was determined to be 2.6 days, which suggests that  $\sim 140$  viral replication cycles occur each year, about half the number estimated by Coffin (19).

It is now apparent that the repetitive replication of HIV-1 (left side of Fig. 2) accounts for  $\geq 99\%$  of the plasma viruses in infected individuals (1, 2, 19), as well as for the high destruction rate of CD4 lymphocytes. The demonstration of the highly dynamic nature of this cyclic process provides several theoretical principles to guide the development of treatment strategies:

- 1) An effective antiviral agent should detectably lower the viral load in plasma after only a few days of treatment.

- 2) On the basis of previous estimates of the viral dynamics (1, 2) and data on the mutation rate of HIV-1 ( $3.4 \times 10^{-5}$  per base pair per replication cycle) (20) and the genome size ( $10^4$  base pairs), Coffin has cogently argued that, on average, every mutation at every position in the genome would occur numerous times each day (19). The larger turnover rate of HIV-1 described in our study makes this type of consideration even more applicable. Therefore, the failure of the current generation of antiviral agents,

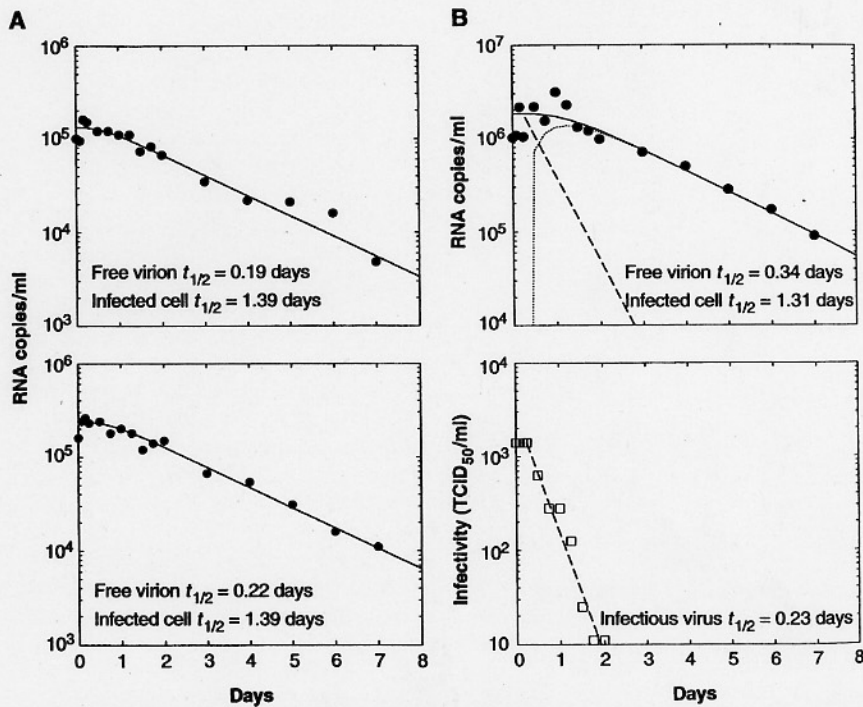


**Fig. 1. (A)** Plasma concentrations (copies per milliliter) of HIV-1 RNA (circles) for two representative patients (upper panel, patient 104; lower panel, patient 107) after ritonavir treatment was begun on day 0. The theoretical curve (solid line) was obtained by nonlinear least squares fitting of Eq. 6 to the data. The parameters  $c$  (virion clearance rate),  $\delta$  (rate of loss of infected cells), and  $V_0$  (initial viral load) were simultaneously estimated. To account for the pharmacokinetic delay, we assumed  $t = 0$  in Eq. 6 to correspond to the time of the pharmacokinetic delay (if measured) or selected 2, 4, or 6 hours as the best-fit value (see Table 1). The logarithm of the experimental data was fitted to the logarithm of Eq. 6 by a nonlinear least squares method with the use of the subroutine DNLS1 from the Common Los Alamos Software Library, which is based on a finite difference Levenberg-Marquardt algorithm. The best fit, with the smallest sum of squares per data point, was chosen after eliminating the worst outlying data point for each patient with the use of the jackknife method. **(B)** Plasma concentrations of HIV-1 RNA (upper panel; circles) and the plasma infectivity titer (lower panel; squares) for patient 105. (Top panel) The solid curve is the best fit of Eq. 6 to the RNA data; the dotted line is the curve of the noninfectious pool of virions,  $V_N(t)$ ; and the dashed line is the curve of the infectious pool of virions,  $V_I(t)$ . (Bottom panel) The dashed line is the best fit of the equation for  $V_I(t)$  to the plasma infectivity data.  $TCID_{50}$ , 50% tissue culture infectious dose.

repetitively when used as monotherapy, is the inevitable consequence of the dynamics of HIV-1 replication. Effective treatment must, instead, force the virus to mutate simultaneously at multiple positions in one viral genome by means of a combination of multiple, potent cyclic pro-antiretroviral agents. Moreover, because the principle process of producing mutant viruses is repeated for ~140 generations each year, early and aggressive therapeutic intervention is

should be

in plasma. It estimates of data on the  $\sim 5$  per base pair have been made (19). The described in consideration of the failure of viral agents.

V<sub>i</sub> declines exponentially [that is,  $V_i(t) = V_0 \exp(-ct)$ , where  $t = 0$  is the time at which the drug takes effect after pharmacokinetic delays]. The existing infectious particles infect cells, and the number of infected cells  $T^*$  varies as given by the solution of Eq. 3, with the initial condition  $T^*(0) = 0$ . At any given time  $t$ , the mean number of virions produced from the initial  $V_0$  virions is  $V_{NI}(t) = P(t)V_0$ , where  $P(t)$  is the (cumulative) probability that a virion is produced by time  $t$ . The probability density of a virus being produced at time  $t$  is  $p(t) = dP/dt$ , and thus the average virion production time  $\tau = \int_0^\infty tp(t)dt$ . Hence,  $\tau = (1/V_0) \int_0^\infty t(dV_{NI}/dt)dt = (1/V_0) \int_0^\infty tN\delta T^* dt$ . Substituting the solution of Eq. 3 for  $T^*$  and integrating yields  $\tau = [(1/\delta) + (1/c)]$ . Because the system is at steady state (10),  $c = NkT_0$ , thus the clearance rate and the rate of new cell infection are coupled. Thus, the viral generation time can also be viewed as the time for an infected cell to produce  $N$  new virions—that is, its life-span ( $1/\delta$ ) plus the time for this cohort of  $N$  virions to infect any of the  $T_0$  uninfected target cells [ $1/(NkT_0)$ ].

**Table 2.** Summary of virion life-span ( $1/c$ ) and infected cell life-span ( $1/\delta$ ), duration of the viral life cycle ( $S$ )

and of the intracellular phase [ $S - (1/c)$ ], and average viral generation time ( $\tau$ ) for the five patients. The values for  $S$  and for the minimal estimate of  $S - (1/c)$  were obtained by a heuristic procedure and should be viewed as rough estimates ( $S$  was estimated by the length of the shoulder on graphs of RNA copies versus time, as in Fig. 1). Confidence intervals for  $\tau$  were obtained by a bootstrap method on a model with  $\tau$  and  $1/\delta$  as parameters. SDs reflect the differences between patients and not the accuracy of the estimates. The fate of a large population of virions was followed to estimate the in vivo value of  $\tau$ . For a system in quasi steady state, the average generation time can be defined as the time required for  $V_0$  particles to produce the same number of virions in the next generation. After a protease inhibitor is administered, all newly produced virions are assumed to be noninfectious. To keep track of the number of noninfectious particles, we assumed for the purposes of this calculation that noninfectious particles are not cleared and act as a perfect marker, recording the production of virions after one round of infection. Thus, from Eq. 5,  $dV_{NI}/dt = N\delta T^*$ . We also assumed that before the drug is given, there are no infected cells [that is,  $T^*(0) = 0$ ], so that only new infections are tracked. Under these circumstances,  $\tau$  is the average time needed for  $V_0$  virions to produce  $V_0$  noninfectious particles after ritonavir administration. After treatment, no further infectious particles are produced and hence the number of infectious particles

necessary if a marked clinical impact is to be achieved (21).

3) From our study and previous reports (1, 2, 5), it is now clear that the "raging fire" of active HIV-1 replication (left side of Fig. 2) could be put out by potent antiretroviral agents in 2 to 3 weeks. However, the dynamics of other viral compartments must also be understood. Although they contribute  $\leq 1\%$  of the plasma virus, each viral

compartment (right side of Fig. 2) could serve as the "ember" to reignite a high rate of viral replication when the therapeutic regimen is withdrawn. In particular, we must determine the decay rate of long-lived, virus-producing populations of cells such as tissue macrophages, as well as the activation rate of cells latently carrying infectious proviruses. This information, someday, will enable the design of a treatment regimen to block de novo HIV-1 replication for a time sufficient to permit each viral compartment to "burn out."

## REFERENCES AND NOTES

- D. D. Ho et al., *Nature* 373, 123 (1995).
- X. Wei et al., *ibid.*, p. 117.
- M. A. Nowak et al., *ibid.* 375, 193 (1995).
- D. J. Kempf et al., *Proc. Natl. Acad. Sci. U.S.A.* 92, 2484 (1995).
- M. Markowitz et al., *N. Engl. J. Med.* 333, 1534 (1995).
- C. Pachl et al., *J. Acquired Immune Defic. Syndr.* 8, 446 (1995); Y. Cao et al., *AIDS Res. Hum. Retroviruses* 11, 353 (1995).
- D. L. Winslow and M. J. Otto, *AIDS* 9 (suppl. A), S183 (1995).
- The rate of virion production is expressed as the product  $N\delta$  to convey either of two possibilities: (i) HIV-1 is produced continuously at an average rate given by the total production of virus particles,  $N$ , divided by the cell life-span,  $1/\delta$ ; or (ii)  $N$  virions are produced in lytic bursts occurring at the rate of cell death,  $\delta$ .
- The effect of a nonperfect drug can be modeled by simply adding the term  $(1 - \eta)\delta N\delta T^*$  to Eq. 4 and multiplying the first term in Eq. 5 by the factor  $\eta$ , where  $\eta$  represents the drug's inhibitory activity [for example,  $\eta = D/(D + EC_{50})$ , where  $D$  is the plasma concentration of drug and  $EC_{50}$  is the concentration required for 50% effectiveness].
- In quasi steady state,  $dT^*/dt = 0$  and  $dV/dt = 0$ . Thus,  $kV_0 T_0 = \delta T_0$  and  $N\delta T_0 = cV_0$ , where the subscript 0 indicates a steady-state value. Combining these equations yields  $NkT_0 = c$ . Each virion infects cells at rate  $kT_0$ , with each infection leading on average to the production of  $N$  new virions. At steady state, the production of new virions at rate  $NkT_0$  must balance the virion clearance at rate  $c$ .
- Equation 6 differs from  $V(t) = [V_0/(c - \delta)][c \exp(-\delta t) - \delta \exp(-ct)]$ , the equation introduced by Wei et al. (2) for analysis of the effects of drug treatment on viral load. Their analysis was based on Eqs. 1 and 2 and the assumption that no new infections occur after drug treatment ( $k = 0$  after treatment). Equation 6 is a new model appropriate for protease inhibitors, which do not prevent infections arising from preexisting mature infectious virions. Because of the symmetry between  $c$  and  $\delta$  in the Wei et al. equation, the virion clearance rate cannot be distinguished from the infected cell death rate by data fitting.
- Because our parameter estimates are based on the assumption of complete inhibition of the production of new infectious virions and no increase in target cells, we expect our parameter estimates to be minimal estimates. Generalizing our model to relax these two assumptions, we can show that  $\delta$  is always a minimal estimate and that, with target cell growth,  $c$  is typically a minimal estimate. We tested how the estimates of  $c$  and  $\delta$  depend on the assumption that ritonavir is 100% effective as follows: We generated viral load data assuming different drug effectivenesses with  $c = 3$  and  $\delta = 0.5$ . With these "data," we used our fitting procedure to estimate  $c$  and  $\delta$  under the assumption that the drug is 100% effective. For data generated with  $\eta = 1.0, 0.99, 0.95$ , and  $0.90$ , we estimated  $c = 3.000, 3.003, 3.015$ , and  $3.028$ , respectively, and  $\delta = 0.500, 0.494, 0.470$ , and  $0.441$ , respectively. Thus, our estimate of  $c$  remains essentially unchanged, whereas that of  $\delta$  is a slight underestimate (for example, for  $\eta = 0.95$ ,  $\delta = 0.47$  rather than the true 0.5). Consequently, if a

Patient	$1/c$ (days)	$1/\delta$ (days)	$S$ (days)	$S - (1/c)$ (days)	$\tau$ (days)
102	0.3	3.8	1.2	0.9	4.1
103	0.4	1.5	1.0	0.6	1.8
104	0.3	2.0	1.2	0.9	2.3
105	0.5	1.9	1.3	0.8	2.4
107	0.3	2.0	1.2	0.8	2.3
Mean	0.3	2.2	1.2	0.9	2.6
$\pm SD$	0.1	0.8	0.1	0.1	0.8

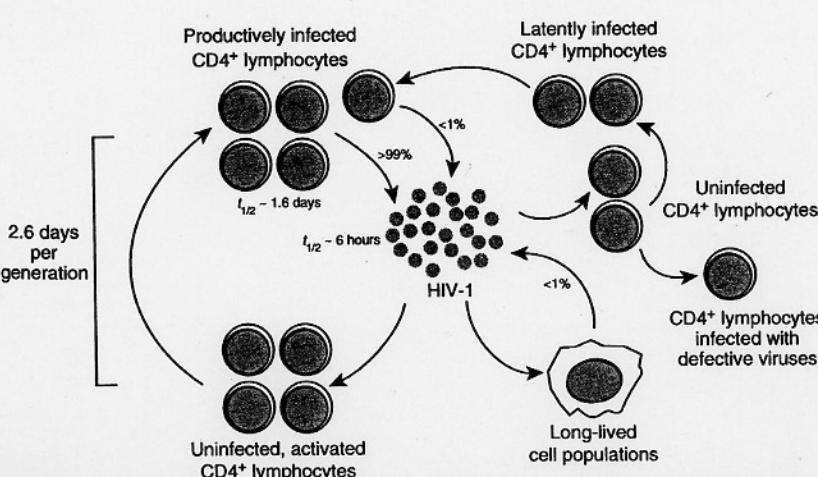


**Fig. 2.** Schematic summary of the dynamics of HIV-1 infection in vivo. Shown in the center is the cell-free virion population that is sampled when the viral load in plasma is measured.

representative data. The load) were in Eq. 6 to hours as the of Eq. 6 by Los Alamos best fit, with a point for open panel; solid curves ions,  $V_{NI}(t)$ ; d line is the tious dose.

drug is not completely effective, cell life-spans may be somewhat less than we estimate. If the target cells are allowed to increase by the maximum factor observed in the five patients (that is, fivefold), we find that the derived values of  $c$  and  $\delta$  are minimal estimates. Thus, for example, for data generated with  $\eta = 1$ , with  $c = 3.00$  and  $\delta = 0.500$ , we find that our fitting procedure yields estimates of  $c = 2.76$  and  $\delta = 0.499$ .

13. D. D. Ho, T. Moudgil, M. Alam, *N. Engl. J. Med.* **321**, 1621 (1989).
14. Virions that are not released into the extracellular fluid are not included in this estimate. Thus, the total production in the body is even larger.
15. The solution to Eq. 3 is

$$T^*(t) = \frac{T_0^*}{c - \delta} [c \exp(-\delta t) - \delta \exp(-ct)] \quad (7)$$

If cellular RNA data were obtained, this equation could be fitted to those data, and the parameter estimates for  $c$  and  $\delta$  could be verified for consistency with the viral kinetics.

16. In principle, more accurate estimates of the duration of the intracellular or eclipse phase of the viral life cycle can be obtained with a model that explicitly includes a delay from the time of infection until the time of viral release. For example, Eq. 2 can be replaced by

$$dV/dt = N\delta \int_0^\infty T^*(t-t')\omega(t')dt' - cV \quad (8)$$

where  $\omega(t')$  is the probability that a cell infected at time  $t-t'$  produces virus at time  $t$ . Explicit solutions to our model, with  $\omega(t')$  given by a gamma distribution, will be published elsewhere (A. S. Perelson et al., in preparation). Alternatively, if virally producing cells  $T_p$  rather than infected cells  $T^*$  are to be tracked, Eq. 1 can be replaced by

$$\frac{dT_p}{dt} = kT \int_0^\infty V(t-t')\omega(t')dt' - \delta T_p \quad (9)$$

- Models of this type can also be solved explicitly when  $\omega(t')$  is given by a gamma function. M. Nowak and A. Herz (personal communication) have solved this model for the case where  $\omega(t')$  is a delta function, in which case the delay simply adds to the pharmacologic delay and Eq. 6 is regained after this combined delay. Analysis of current data by nonlinear least squares estimation has so far not allowed accurate simultaneous estimation of  $c$ ,  $\delta$ , and the intracellular delay. However, the qualitative effect of including the delay in the model is to increase the estimate of  $c$ , which is consistent with our claim that the values of  $c$  in Table 1 are minimal estimates. Higher values of  $c$  (hence lower values of  $1/c$ ) will lead to increased estimates of the intracellular delay,  $S - (1/c)$ . Thus our estimate of the duration of the intracellular phase, as derived above and given in Table 2, is still a minimal estimate.
17. A. Carmichael, X. Jin, P. Sissons, L. Borysiewicz, *J. Exp. Med.* **177**, 249 (1993).
  18. N. Nathanson and B. Harrington, *Am. J. Epidemiol.* **85**, 494 (1966).
  19. J. M. Coffin, *Science* **267**, 483 (1995).
  20. L. M. Mansky and H. M. Temin, *J. Virol.* **69**, 5087 (1995).
  21. D. D. Ho, *N. Engl. J. Med.* **333**, 450 (1995).
  22. B. Efron and R. Tibshirani, *Stat. Sci.* **1**, 54 (1986).
  23. We thank the patients for participation; A. Hurley, Y. Cao, and scientists at Chiron for assistance; B. Goldstein for the use of his nonlinear least squares fitting package; and G. Bell, T. Kepler, C. Macken, E. Schwartz, and B. Sulzer for helpful discussions and calculations. Portions of this work were performed under the auspices of the U.S. Department of Energy. Supported by Abbott Laboratories, grants from NIH (NO1 AI45218 and RR06555) and from the New York University Center for AIDS Research (AI27742) and General Clinical Research Center (MO1 RR00096), the Aaron Diamond Foundation, the Joseph P. Sullivan and Jeanne M. Sullivan Foundation, and the Los Alamos National Laboratory Directed Research and Development program.

10 October 1995; accepted 29 January 1996

## Opposite Modulation of Cocaine-Seeking Behavior by $D_1$ - and $D_2$ -Like Dopamine Receptor Agonists

David W. Self,\* William J. Barnhart, David A. Lehman, Eric J. Nestler

Activation of the mesolimbic dopamine system is known to trigger relapse in animal models of cocaine-seeking behavior. We found that this "priming" effect was selectively induced by  $D_2$ -like, and not by  $D_1$ -like, dopamine receptor agonists in rats. Moreover,  $D_1$ -like receptor agonists prevented cocaine-seeking behavior induced by cocaine itself, whereas  $D_2$ -like receptor agonists enhanced this behavior. These results demonstrate an important dissociation between  $D_1$ - and  $D_2$ -like receptor processes in cocaine-seeking behavior and support further evaluation of  $D_1$ -like receptor agonists as a possible pharmacotherapy for cocaine addiction.

Relapse of cocaine use in cocaine-dependent people is often precipitated by episodes of intense drug craving even after prolonged abstinence. Cocaine craving has been described subjectively as resembling the positive or "high"-like qualities of the drug itself (1). In this sense, cocaine craving may differ from cravings for opiates or ethanol, which are sometimes described as a desire to alleviate the negative, withdrawal-associated symptoms of drug dependence (1). Both cocaine craving in humans and relapse in animal models of cocaine-seeking behavior are triggered by environmental stimuli associated with the drug experience (2, 3) and by low doses of cocaine itself (3, 4).

The priming effects of such cues in animal models of cocaine-seeking behavior can be mimicked by activation of the mesolimbic dopamine system (5), which is a major neural substrate of cocaine reinforcement (6). Dopamine acts at two general classes of dopamine receptors, termed  $D_1$ -like and  $D_2$ -like, that are distinguishable by their structural homology (7), opposite modulation of adenylate cyclase activity (8), and differential localization within the brain (9).

We tested the ability of full  $D_1$ - or  $D_2$ -like dopamine receptor agonists to induce relapse in an animal model of cocaine-seeking behavior. Male Sprague-Dawley rats were trained to press a lever to self-administer intravenous cocaine (10, 11). A daily 4-hour reinstatement procedure was followed in which rats self-administered cocaine for 2 hours, after which saline was substituted for the cocaine during the final 2 hours. During the time that saline was substituted, the rats' "nonreinforced" lever-press responses progressively diminished, a behavioral phenomenon known as extinction.

Laboratory of Molecular Psychiatry, Departments of Psychiatry and Pharmacology, Yale University School of Medicine, Connecticut Mental Health Center, New Haven, CT 06508, USA.

\*To whom correspondence should be addressed.

tion. After responding had diminished (1), the rats were given intraperitoneal priming injections of either the  $D_2$ -like selective receptor agonists 7-hydroxy-N,N-di-n-propyl-2-aminotetralin (7-OH-DPAT) (12) or quinpirole (13), or the  $D_1$ -like selective receptor agonist SKF 82958 (14). Although these dopamine agonists can selectively discriminate the  $D_1$ - from the  $D_2$ -like class of receptors, they do not adequately distinguish the various subtypes within each class in vivo. The priming ability of these dopamine receptor agonists was assessed by the ability to reinstate nonreinforced lever-pressing for saline infusions at the lever previously delivered cocaine infusions (drug-paired lever) during the cocaine phase of the test session (Fig. 1).

The  $D_2$ -like agonist 7-OH-DPAT produced large dose-related increases in nonreinforced responding at the drug-paired lever as compared with very low levels of responding induced both by the drug vehicle and at an inactive lever (Figs. 1 and 2). Quinpirole also induced selective responding at the drug-paired lever and with higher potency but with less efficacy and dependency than responding induced by 7-OH-DPAT. These differences cannot be explained by the relative selectivity or affinity of the two agonists at  $D_2$  or  $D_3$  receptor subtypes (12) and therefore probably reflect different pharmacokinetic properties of the drugs. The possibility of a general rate-increasing effect of the  $D_2$ -like agonist is eliminated by the lack of significant responding at the inactive lever and by previous studies in which  $D_2$ -like agonists produced decreases rather than increases in responding when animals were treated during cocaine self-administration tests (15, 16). Thus, we conclude that the  $D_2$ -like agonists initiate neural processes that trigger relapse in an animal model of cocaine-seeking behavior.

In contrast to the  $D_2$ -like agonists,